Research article

High copy arrays containing a sequence upstream of mec-3 alter cell migration and axonal morphology in C. elegans

Nicole Toms, Jennifer Cooper, Brandi Patchen and Eric Aamodt*

Address: Louisiana State University Health Sciences Center-Shreveport, Department of Biochemistry and Molecular Biology, Shreveport, USA

E-mail: Nicole Toms - eaamod@lsuhsc.edu; Jennifer Cooper - repooc730@aol.com; Brandi Patchen - bpatch@lsuhsc.edu; Eric Aamodt* - eaamod@lsuhsc.edu
*Corresponding author

Published: 31 January 2001

BMC Developmental Biology 2001, 1:2

Received: 22 November 2000
Accepted: 31 January 2001

This article is available from: http://www.biomedcentral.com/1471-213X/1/2

Abstract

Background: The *Caenorhabditis elegans* gene *mec-3* encodes a LIM-homeodomain protein that is a master regulator of touch receptor neuron genes. Two of the touch neurons, the ALM neurons, are generated in the anterior of the animal and then migrate to near the middle of the animal. In animals transformed with a sequence upstream of *mec-3*, the ALM touch receptor neurons failed to migrate to their normal positions and sometimes migrated in the wrong direction, and the PLM touch receptor neurons showed axonal defects. Here we characterize this effect and identify the sequence causing the cell migration and axonal defects.

Results: The ALM migration defect did not result from RNA interference (RNAi), nonspecific effects of carrying a transgenic array, expression of GFP, or the marker gene used to make the transformants. Instead, the ALM migration defect resulted from transgenic arrays containing many copies of a specific 104 bp DNA sequence. Transgenic arrays containing this sequence did not affect all cell migrations.

Conclusions: The *mec-3* upstream sequence appeared to be sequestering (titrating out) a specific DNA-binding factor that is required for the ALMs to migrate correctly. Because titration of this factor could reverse the direction of ALM migrations, it may be part of a program that specifies both the direction and extent of ALM migrations. *mec-3* is a master regulator of touch receptor neuron genes, so the factor or factors that bind this sequence may also be involved in specifying the fate of touch receptor neurons.

Background

Cell migration is one of the most important and complex cellular behaviors. It is essential for animal development, immune system function, and wound repair. Defects in cell migration can lead to human diseases such as birth defects, and failure to control cell migration is an important step in tumor metastasis.

We currently believe that migrating cells extend and retract actin rich protrusions, lamellipodia and filopodia, into their environment. Protrusions that adhere strongly enough are stabilized and fail to retract. In this way, cells (or cell processes) can follow adhesive guidance cues. While this model has been around for some time [1], we are only now beginning to understand the molecular signals that cause cells to initiate movement, how cells

move, the signals that guide the cell migrations, and the signals that stop cells at their appropriate positions.

Recently, progress in understanding cell migration has come from studies of *Caenorhabditis elegans* and *Drosophila* [2]. Most cell migration genes identified in these simple invertebrates are conserved in vertebrates, which confirms the efficacy of these genetically tractable systems for studying cell migration.

C. elegans is a particularly attractive system for the study of cell migration. These animals are transparent and anatomically simple, so cell migrations can be followed in the living animal at all stages of development by fluorescence microscopy of GFP fusion proteins or by Nomarski microscopy. Both the cell lineage and the cell migrations are invariant from animal to animal, so migration defects can be easily identified.

Several genetic screens performed with *C. elegans* have identified mutations that interfere with cell migrations (for reviews see [2, 3]). Some of these mutations affect all cell migrations, whereas others only affect the migrations of a limited subset of cells. Not surprisingly, many of these mutants also show defects in axon extension, bundling and pathfinding. The genes identified by these mutations encode extracellular proteins, cell surface receptors, fibroblast growth factor-like proteins and their receptors, adhesion molecules, small GTPases, non-muscle myosins and transcription factors.

In *C. elegans*, three genes, *unc*-6, *unc*-5 and *unc*-40, guide cells and processes along the dorsal-ventral axis [4]. All of these genes are conserved across broad groups of animals from *C. elegans* to man. UNC-6 protein, a laminin-like protein that is located in the ventral region of the animal, is a homolog of the vertebrate protein netrin. UNC-5 and UNC-40 are cell surface receptors that interact with UNC-6. UNC-5 promotes dorsal migrations, whereas UNC-40 promotes ventral migrations, both in response to UNC-6 signals. Based on studies in other species, the difference in how UNC-5 and UNC-40 guide cells and axons lies in their intracellular domains [5, 6].

Mutations in *unc-129*, a member of the transforming growth factor β (TGFβ) superfamily, were identified as genetic suppressors of ectopic UNC-6 signaling [7]. *unc-129* is expressed dorsally and loss of UNC-129 function disrupts dorsal axon migrations. In *Drosophila*, TGFβ family members are also involved in controlling dorsal-ventral migrations [8]. It appears, therefore, that the UNC-6/netrin and TGFβ guidance systems act redundantly and are conserved across species.

The guidance of cells and axons along the anterior-posterior axis of *C. elegans* is not as well understood. Two genes involved in anterior-posterior cell migration are *vab*-8 and *mig-13*. VAB-8 is a kinesin-related protein that acts cell autonomously and is involved in posterior cell migrations [9, 10]. Therefore, VAB-8 is probably involved in the cellular response to guidance cues. MIG-13 is a novel transmembrane protein that acts non-cell autonomously and is involved in anterior cell migrations [11, 12]. The dose of MIG-13 appears to affect the extent of anterior cell migrations [12]. MIG-13 may, therefore, signal to cells their direction and extent of migration.

Chalfie and colleagues have identified a transcriptional cascade that leads to the activation of touch neuron-specific genes. UNC-86 is a POU homeodomain transcription factor needed to activate the *mec-3* gene [13,14,15]. *mec-3* in turn encodes a LIM homeodomain protein that is expressed in the six touch receptor neurons, two FLP neurons and two PVD neurons. MEC-3 and UNC-86 proteins form a heterodimer that binds to and activates the *mec-3* promoter and the promoters of touch receptor-specific genes such as *mec-7* and *mec-4* [13,14,15]. In this way, MEC-3 activates its own transcription, which probably prevents the dedifferentiation of the touch neurons. Later in development, *mec-17* also contributes to the maintenance of *mec-3* expression [16].

We show here that a sequence upstream of *mec-3*, when transformed into *C. elegans* in high copy arrays, altered the extent and direction of ALM touch receptor neuron migrations. This sequence also disrupted extension of the PLM touch receptor axon. These defects did not result from RNA interference (RNAi), the heavy genetic load of carrying a transgenic array, the expression of GFP, or the *rol-6* marker gene used to make the transgenic arrays. The ALM migration defects were due to a specific DNA sequence and only occurred when there were many copies of that sequence in the array. This sequence did not affect all cell migrations, the ALM/BDU cell division or the positions of the BDU cells. We conclude, therefore, that the sequence is sequestering a factor that helps control ALM migrations and PLM axon outgrowth. We also suggest that this factor may be differentially segregated into touch receptor neurons and that it may help specify the touch receptor neuron cell fate.

Results

The ALM touch receptor neurons are the lineal sisters of the BDU neurons [17]. The ALMs are generated anterior to the BDUs but then migrate posteriorly to near the middle of the animal, while the BDUs migrate anteriorly a short distance (Figure 1A) [12]. While looking for the DNA element that mediates the PAG-3 dependent suppression of *mec-3* in the BDU neurons [18, 19], we iden-

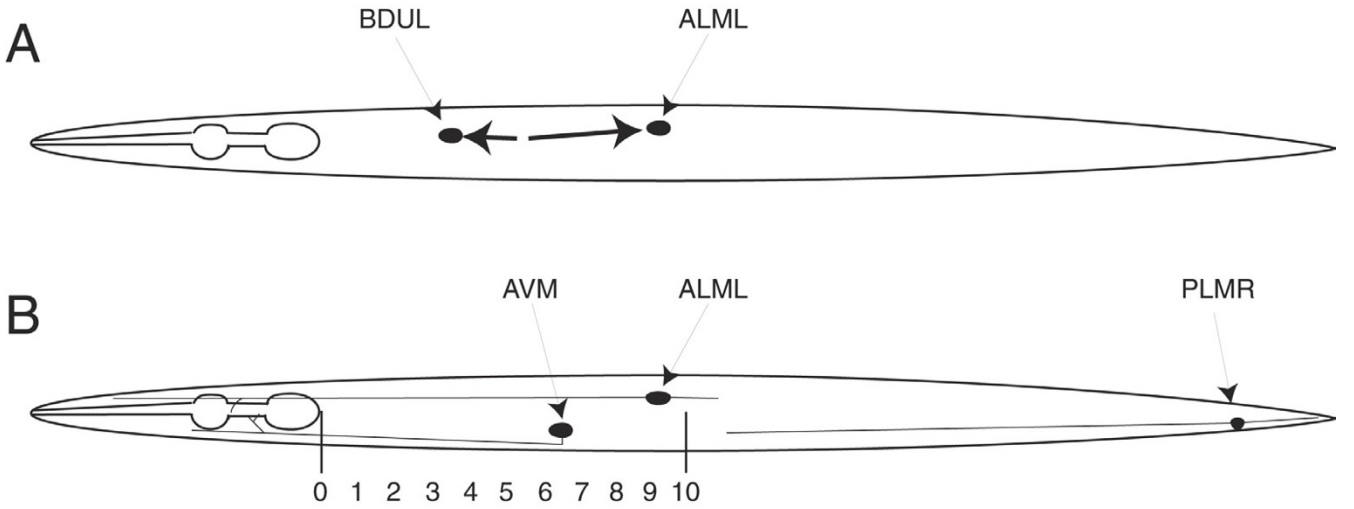

Figure 1
A. Origin and migration of the BDU and ALM neurons. The ALM touch receptor neurons and the BDU interneurons are lineal sisters (the AB.arpppapp and AB.arppaapp cells divide to give ALMR/BDUR and ALML/BDUL, respectively). The ALMs are generated anterior to the BDUs but migrate posteriorly, while the BDUs migrate anteriorly so that each cell stops near the positions shown. B. Position and axonal morphology of the ALM, AVM and PLM touch receptor neurons. The scale shown at the bottom was used to measure ALM, BDU and AVM positions in the experiments shown below. The ALMs are located around position 9, the AVMs are located between positions 6 and 7 and the BDUs are located between positions 3 and 4 in wild type animals.

tified extrachromosomal arrays that alter ALM touch neuron migration. In animals containing these arrays, the ALM touch neurons are found anterior to their normal positions. Some ALMs even migrated anteriorly rather than posteriorly with final positions anterior to where they originated.

To measure the ALM migration defect in strains containing these arrays, we conceptually divided the region of the animal from the rear bulb of the pharynx to the middle of the animal into 10 sections, identified as positions 1-10 (Figure 1B), and visually scored ALM positions along this scale. The normal positions of ALMs would be between 8 and 10 on this scale.

ALM migration and PLM axonal morphology defects

Figure 2 shows fluorescence micrographs and bar graphs of the positions of the ALMs from strain TU2562, which has an integrated *mec-3gfp* (equivalent to pJC8 in Figure 4), and strain EA485, which contains a high copy extrachromosomal array made from plasmid pJC4 (see Figure 4 and Materials and Methods). In strain TU2562, the ALMs migrated close to their normal positions; the average position was 8.6 (n=190) on the scale described above. In EA485, the ALMs were usually anterior to their normal positions; the average position was 4.2 (n=175) on this scale.

Strains that showed the ALM migration defects also showed defects in another pair of touch neurons, the PLMs. Figure 3 shows an example of a normal PLM in strain TU2562 and several examples of PLMs with axonal defects in strain EA485. All of the 189 PLMs scored in TU2562 had normal morphology, whereas 64% of the 183 PLMs scored in EA485 had defects in axonal morphology. In EA485, the PLM axons were often short, misdirected and had extra branches.

Axonal defects in the ALMs were less common than in the PLMs. In EA485, 77.4% of 199 ALMs scored had normal axonal morphology, whereas in TU2562, all of the 117 ALMs scored had normal morphology. The majority of ALMs with abnormal axonal morphology were in positions 1-3 with a few as posterior as position 5. All ALMs located posterior to position 5 had normal axonal morphology.

The ALM migration defect was due to a specific DNA sequence

To determine whether the ALM migration defect was due to the presence of a specific DNA sequence in the extrachromosomal arrays, we generated *mec-3gfp* deletion constructs containing various portions of the *mec-3* upstream sequences. Plasmids pJC8, pJC3, pJC4, pJC1, pJC18 and pJC19 were made as described in Materials and Methods and plasmid pPD118.17 was a gift from A. Fire. We transformed these plasmids into wild type animals as described in Materials and Methods and screened for transgenic lines. All of the resulting strains expressed *mec-3gfp* in the ten cells where *mec-3* is nor-

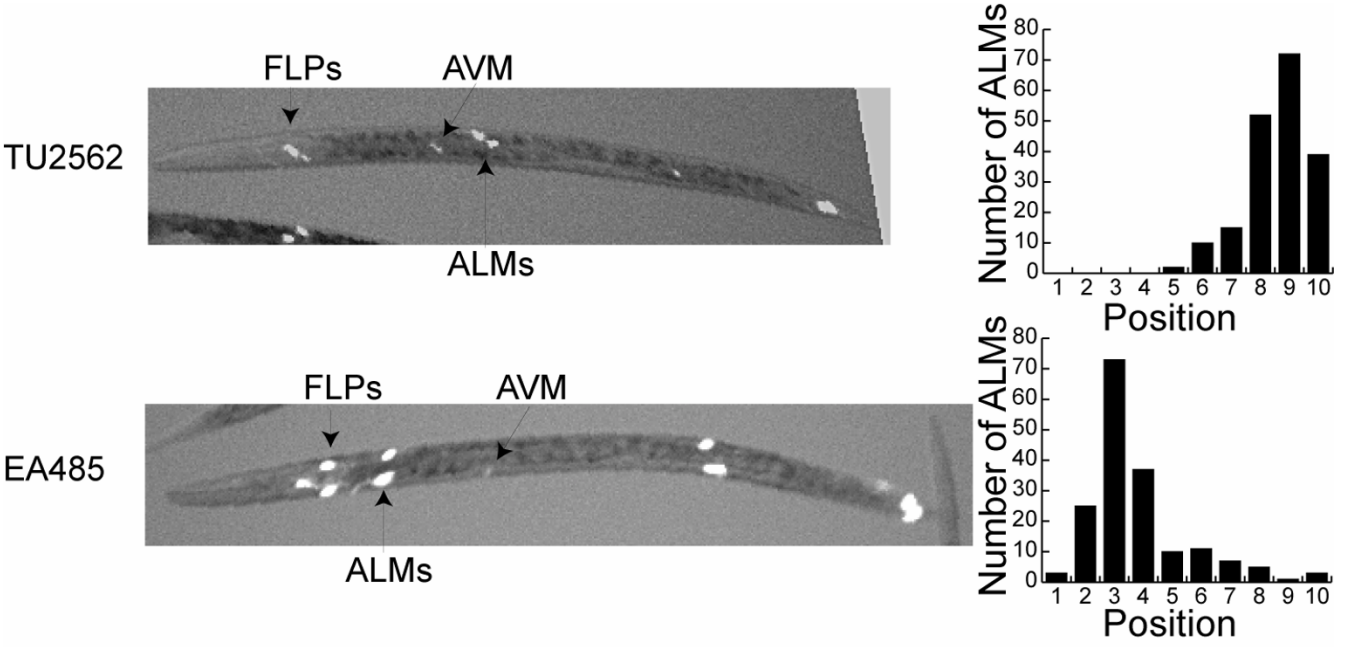

Figure 2
ALM positions in lines TU2562 and EA485. Micrographs on the left show examples of the positions of the FLPs, AVM and ALMs in TU2562 and EA485. The animals are positioned with anterior to the left. White areas are cells expressing green fluorescent protein. Bar graphs on the right show the number of ALMs at each position in 100 animals from each strain. The ALM positions in TU2562 were similar to those in wild type animals whereas the ALMs in EA485 were located significantly anterior to their normal positions. The system for scoring ALM positions is described in Figure 1.

mally expressed. We measured the ALM positions in 100 animals from each strain.

Figure 4 shows the region of *mec-3gfp* included in each of the plasmids, the combined distribution of ALM positions from three strains transformed with each construct, the percent of ALMs that showed migration defects (those located anterior to position 8) and the total number of ALMs scored. Strains transformed with pJC8, pJC3, and pJC4 showed strong ALM migration defects but strains transformed with plasmids pPD118.17 and pJC1 showed few ALM migration defects. The region from *Pst*I to *Bbs*I appeared to suppress the migration defect (compare pJC3 to pJC4). The 495 bp region from the 5' end of the *mec-3* clone to the *Pst*I site appeared to most strongly affect ALM migrations (compare pJC3 and pJC4 to pPD118.17 and pJC1). Further deletions of this region (pJC18 and pJC19) resulted in less severe migration defects. These data and results described below are consistent with the hypothesis that this sequence contains multiple binding sites that titrate out a cell migration factor or factors. Below we refer to this sequence as the titrating sequence.

The migration defect was not due to nonspecific effects of carrying an array, expression of GFP, or the rol-6 transformation marker gene

The above data also show that the ALM migration and PLM axonal morphology defects are not due to nonspecific effects of carrying an extrachromosomal array. Some arrays such as those made with plasmids pPD118.17 and pJC1 had little effect on ALM migration and PLM axonal morphology.

There have been reports that expression of GFP in neurons can have toxic effects [20, 21]. The above results, however, show that neither the migration defects nor the PLM axonal morphology defects resulted from expression of GFP. Some arrays, such as the integrated array in strain TU2562 and the extrachromosomal arrays containing plasmids pPD118.17 and pJC1, express GFP yet had few ALM migration or PLM axonal morphology defects. The lines transformed with pJC1 had especially bright GFP fluorescence yet had few ALM or PLM defects.

All of the lines shown in Figure 4 were made by co-injection of the plasmid of interest and the plasmid pRF4, which contains the *rol-6(su1006)* marker gene. Because some of these arrays, and others described below, did not

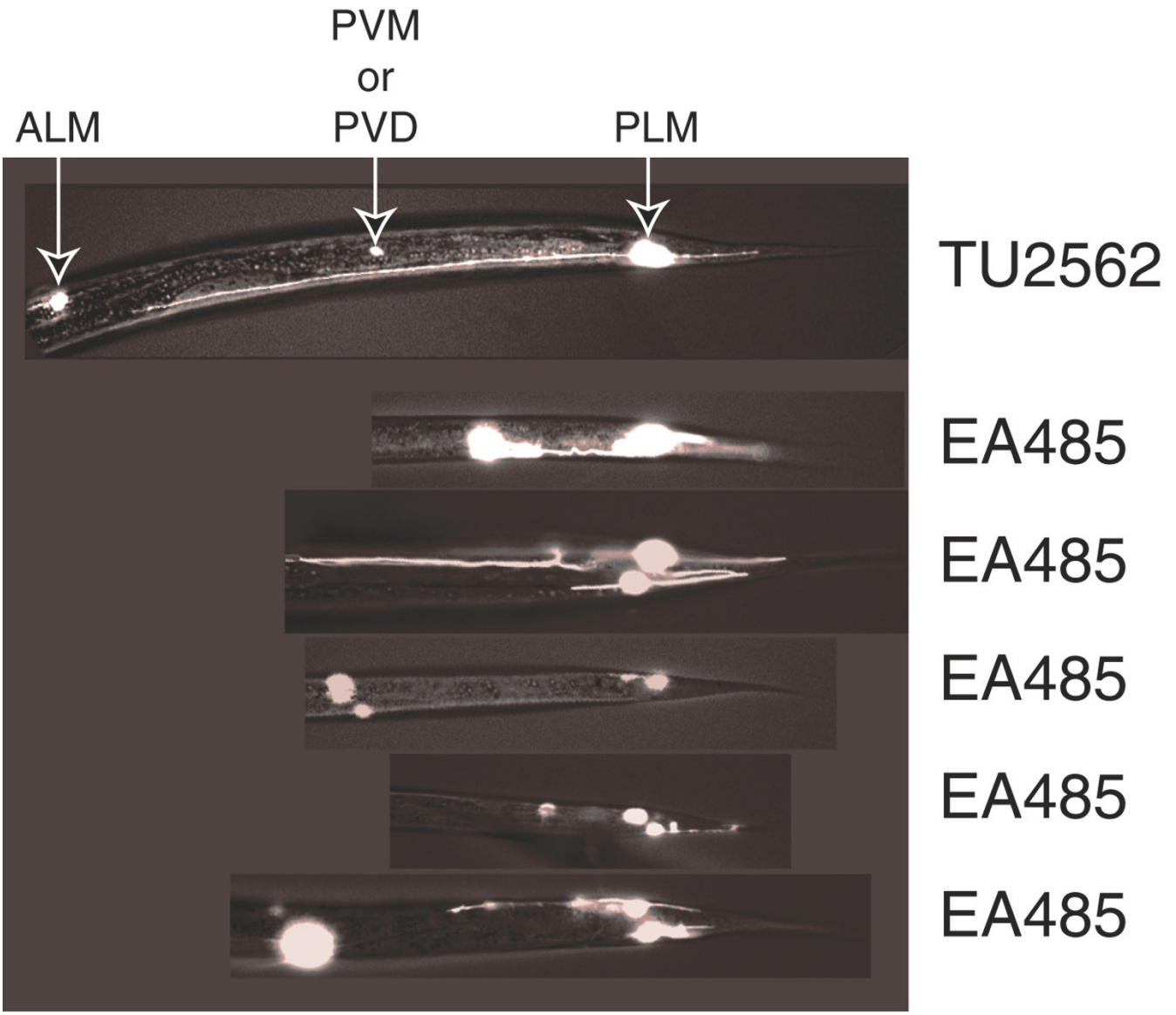

Figure 3
Fluorescence micrographs showing PLM axonal morphology in TU2562 and EA485. The top panel shows a PLM with normal morphology in a TU2562 animal. The next five panels show examples of PLMs with axonal morphology defects in EA485 animals. The white spots anterior to the PLMs are the *mec-3* expressing PVM and PVD neurons.

induce ALM migration or PLM axonal defects, these phenotypes were not due to the *rol-6* marker plasmid.

The ALM migration defect was not due to RNAi

In *C. elegans*, the presence of double stranded RNA that corresponds in sequence to a gene will usually result in silencing of that gene [22]. This effect is referred to as RNA interference or RNAi. In several cases where transgenic arrays induced odd phenotypes, the authors attribute this to RNAi effects resulting from cryptic promoters on either side of the transformed gene [23]. In the case described here, it seemed unlikely that RNAi was inducing the ALM migration or the PLM axonal morphology defects because there is no predicted protein-encoding gene in the titrating sequence. It was conceivable, however, that a small, undetected gene was present in this sequence. To test this possibility, we generated double stranded RNA that corresponded to the sequence 5' of the *Pst*I restriction site and injected it into TU2562 animals. TU2562 was chosen because it expresses GFP in its ALMs and these neurons migrate normally.

In strain TU2562 the average ALM position was 8.6. In two separate experiments, TU2562 injected with double stranded RNA containing the *mec-3* sequence 5' of the

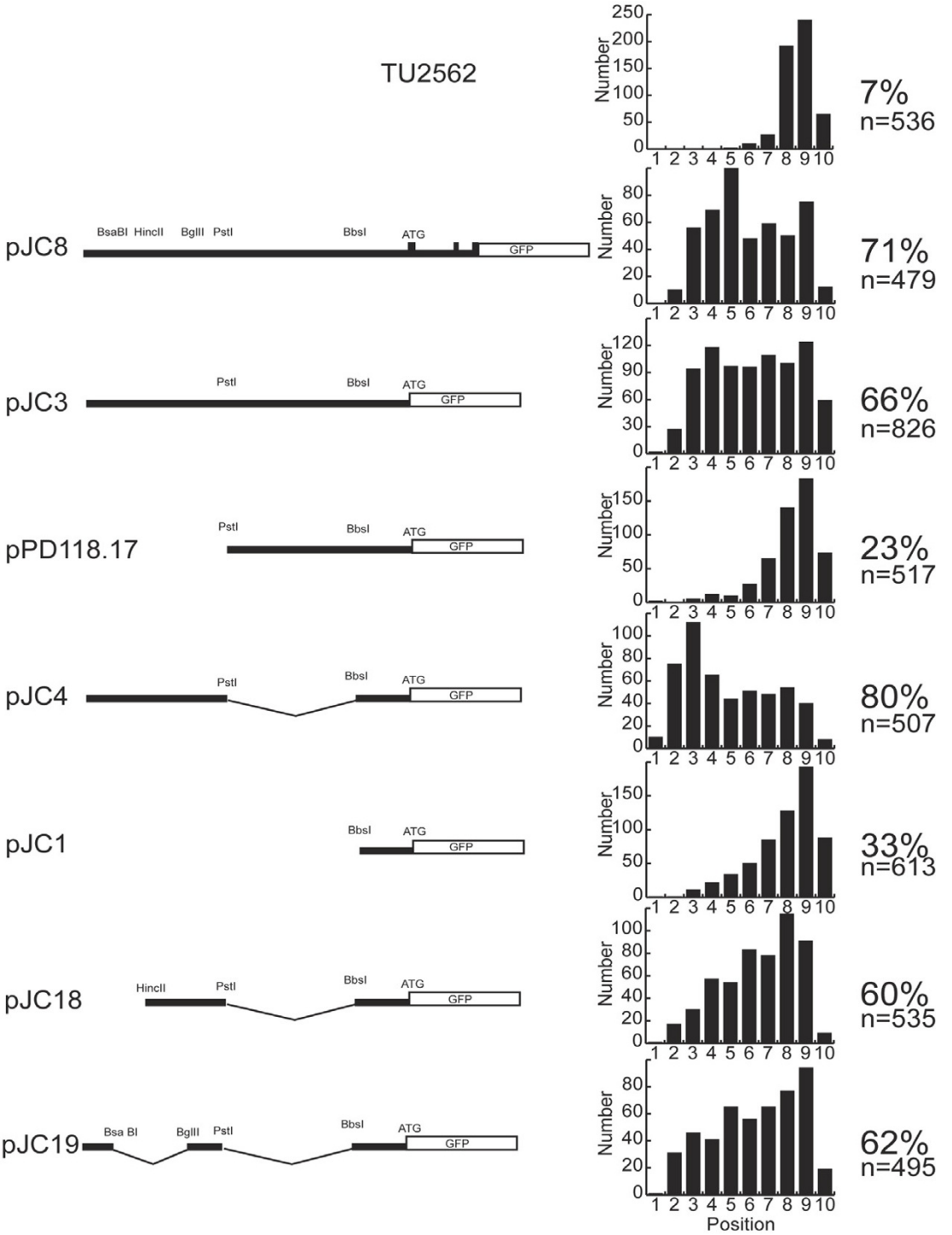

Figure 4
ALM positions in strains transformed with *mec-3* upstream regions. Data from strain TU2562 is included to show the normal distribution of ALMs. The diagrams on the left indicate the regions of *mec-3* in each plasmid. ATG marks the translational start site. *Bsa* BI, *Bgl*II, *Pst*I and *Bbs*I are restriction enzyme cutting sites. Filled rectangles represent *mec-3* exons. The open rectangles marked GFP represent green fluorescent protein encoding sequences. pJC8 begins 2372 bp upstream of the *mec-3* translational start site and is fused to GFP at the end of exon 3. The bar graphs show the number of ALMs at each position. The number of ALMs is on the Y-axes and the position is on the X-axes. For most constructs, 100 animals from each of three separate transgenic lines were scored for ALM positions. For two strains transformed with pJC3, 200 animals were scored. The percent refers to the percent of ALMs anterior to position 8, and n is the total number of ALMs scored. The system for scoring ALM positions is described in Figure 1.

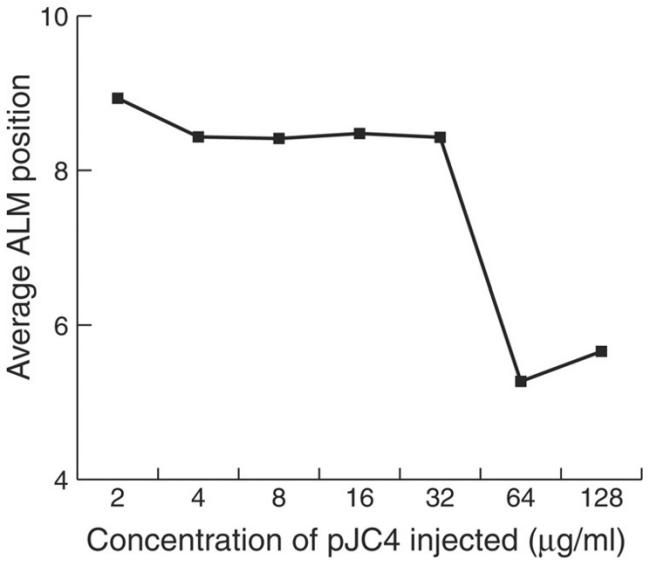

Figure 5
The ALM migration phenotype depended on the amount of pJC4 in the array. Arrays were made with different concentrations of pJC4 as described in Materials and Methods. We measured the positions of ALMs in 100 animals from each strain and calculated the average position.

*Pst*I restriction site also had average ALM positions of 8.6 (n=190 and n=167). These RNA injected animals also had normal PLM axonal morphology. Therefore, the ALM migration and the PLM axonal morphology defects were not due to RNAi.

Many copies of the titrating sequence were required to induce the ALM migration defect

To determine whether the migration defect resulted from having many copies of the titrating sequence, we made transformants with different mixtures of plasmid and genomic DNA. Kelly et al. [24] have shown that blunt end cut plasmids injected with blunt end cut genomic DNA will form complex arrays that contain genomic DNA intermixed with a few copies of the plasmid. To generate arrays with different numbers of copies of pJC4, we co-injected pJC4 plasmid DNA with pRF4 and genomic DNA as described in Materials and Methods. We measured the positions of the ALMs in 100 animals from one transgenic strain made with each DNA mixture.

Figure 5 shows a plot of the average ALM position versus the concentration of pJC4 in the injection mixture. The ALMs were close to their normal positions in the strains made with 2, 4, 8, 16 and 32 µg/ml of pJC4 but showed a clear migration defect at 64 and 128 µg/ml of pJC4.

Does this sequence affect all cell migrations?

The QR.p neuroblast is generated in the posterior of the animal [12, 25]. As shown in Figure 8A, it migrates anteriorly to the middle of the animal where it stops and then

Having a promoter near the titrating sequence did not enhance the ALM migration defect

All of the plasmids shown in Figure 4 contained both the *mec-3* promoter and the GFP encoding sequence. We reasoned that pJC4 may have caused more severe migration defects than pJC8 and pJC3 because in pJC4 the titrating sequence was closer to the promoter and was thereby more accessible to binding factors. To determine whether having a promoter present increased the effectiveness of this sequence, we made two plasmids shown in Figure 6. Plasmid pJC11 had the region upstream of the *Pst*I site fused to the region of the *mec-3* promoter, whereas pJC10 had just the *mec-3* region upstream of the *Pst*I site. We transformed TU2562 with these plasmids and generated transgenic lines. Because the extrachromosomal arrays did not contain *mec-3gfp*, we first picked rollers and then scored them for ALM position. Due to the mosaic inheritance of extrachromosomal arrays, some of the ALMs scored may not have contained the array.

Figure 6 shows the regions of *mec-3* included in each plasmid and the distribution of ALM positions from three separate strains made with each plasmid. On the right are listed the percent of ALMs that showed migration defects and the total number of ALMs scored from the three strains transformed with each construct. Plasmids pJC10 and pJC11 appeared to be equally capable of inducing ALM migration defects.

What is the sequence?

To further refine the region responsible for inducing the ALM migration defect, we generated plasmids containing further deletions of the 495 bp *mec-3* region upstream of the *Pst*I site. We transformed these plasmids into TU2562 and analyzed the ALM positions in the resulting lines as we did for the lines shown in Figure 6. Figure 7 shows the results of this experiment. Arrays containing pJC15 induced migration defects less effectively than arrays containing pJC10 (Fig. 6), so sequences within the *Pst*I to *Bgl*II region appear to contribute to the migration defect. However, the pJC13 data show that arrays containing this sequence by itself induced few migration errors. pJC15 arrays and pJC14 arrays induced similar migration defects, so the sequence from the *Bgl*II to the *Hpa*I restriction sites did not appear to contribute to the migration defect. pJC16 arrays induced fewer migration defects than pJC14 arrays and pJC17 arrays induced fewer migration defects than pJC16 arrays, so there appeared to be multiple sequences between the *Hpa*I and *Bsa*BI restriction sites that contributed to the migration defect.

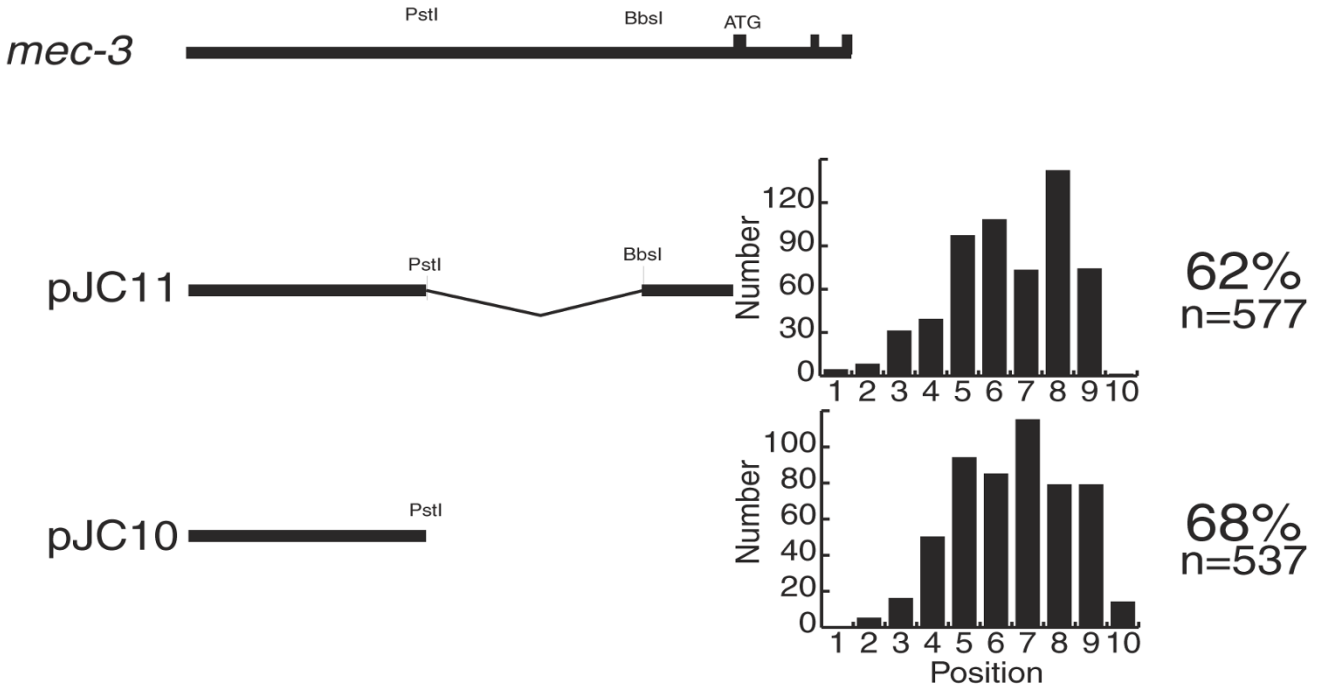

Figure 6
The *mec*-3 promoter did not enhance the titration effect. The sequence from the *Bbs*I site to the *mec*-3 translation start site contained the *mec-3* promoter. Plasmid pJC11, which contained the *mec*-3 promoter, and plasmid pJC10, which did not contain the *mec-3* promoter, were transformed into strain TU2562. Three lines were generated from each plasmid. The bar graphs show the positions of ALMs from 100 animals for each of the three lines. The percent of misplaced ALMs and the number of ALMs scored are shown on the right.

divides. One of the resulting cells, QR.pp, undergoes programmed cell death while the other, QR.pa migrates forward to about position 7 and again stops and divides. QR.pa gives rise to two neurons, SDQR and the AVM touch receptor neuron. Thus, if the transgenic arrays containing the titrating sequence affect all cell migrations, the AVMs should also be misplaced.

To test this idea, we measured the AVM positions in TU2562 and EA485. Figure 8B shows the distributions of AVM positions for these two strains. The average positions of the AVMs in EA485 and in TU2562 were both 6.3. As shown above, the ALMs in TU2562 were near their normal positions, whereas the ALMs in EA485 were grossly misplaced. Clearly, the migrations of the QR.p neuroblast and its daughter, QR.pa, unlike the ALM neurons, were not affected by the extrachromosomal array in EA485.

The ALM migration and the PLM axonal morphology defects are highly correlated

Strains that had many ALM migration defects also had many PLM axonal defects. The correlation coefficient of the average ALM position versus the percent of animals with PLM axonal defects was -0.99. This correlation between the ALM defects and the PLM defects is consistent with both defects resulting from the titration of the same factor or factors.

The titrating sequence did not affect the ALM/BDU cell division or the positions of the BDUs

In strains containing these arrays, some of the ALMs that were anterior to position 6 had an axonal morphology similar to their lineal sisters, the BDU neurons. We wondered whether in these animals the ALM/BDU cell division was not occurring and the progenitor of these neurons was taking on some of the character of both cells. This ALM/BDU cell might migrate anteriorly, like a BDU, and express *mec-3gfp*, like an ALM. To address this, we asked whether the BDU neurons were present in animals where the ALMs were displaced anteriorly. We

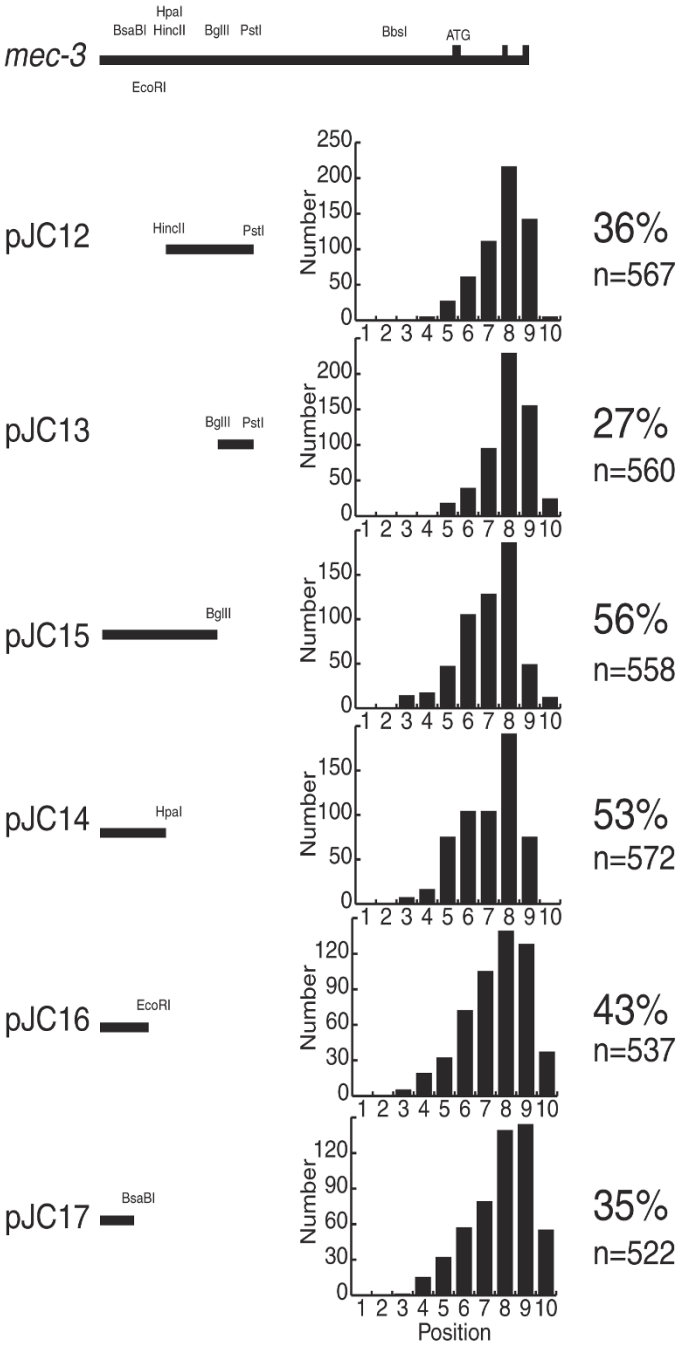

Figure 7
mec-3 upstream sequences that contribute to ALM migration defects. The diagrams on the left indicate the regions of *mec-3* in each plasmid. The top diagram labeled *mec-3* includes sequences from 2400 bp 5' of the *mec-3* translational start site (ATG) through exon 3. *Pst*I, *Hinc*II, *Bgl*II and *Hpa*I indicate restriction enzyme cutting sites. Three lines were generated for each plasmid. The bar graphs show the positions of ALMs from 100 animals for each of the three lines. The percent of misplaced ALMs and the number of ALMs scored are shown on the right.

took advantage of the fact that in *pag-3* mutants, *mec-3gfp* is expressed in both the ALMs and in the BDUs (McDermott, J. et al., unpublished results). We crossed the pJC4 array in EA485 into a *pag-3(ls20)* genetic background to generate strain EA489. As a control, we crossed the integrated array in TU2562 into a *pag-3(ls20)* genetic background to generate strain EA363. In these strains, we measured the positions of the ALMs and BDUs. In a *pag-3(ls20)* background, the BDU neurons have a lower level of *mec-3gfp* expression than the

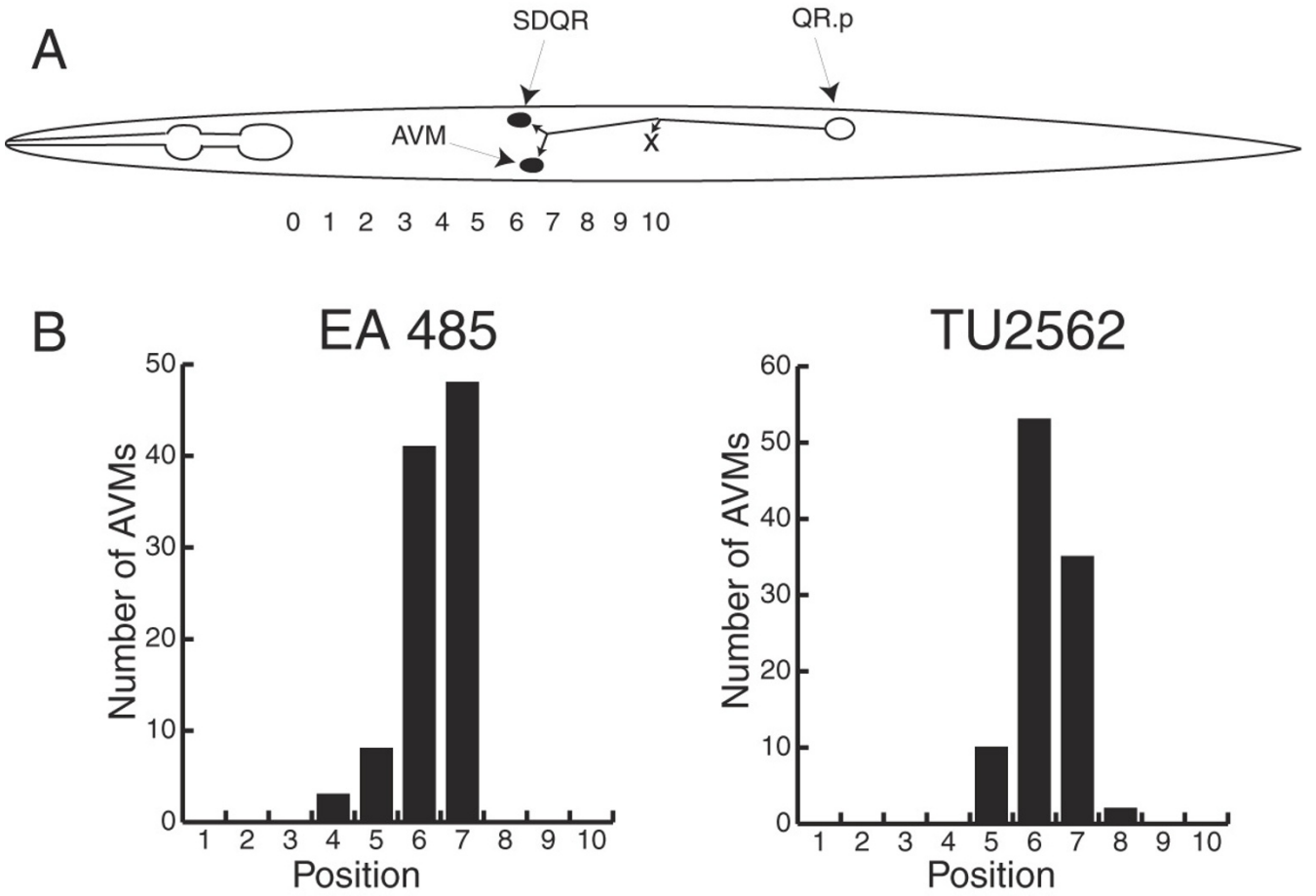

Figure 8
A. Migration of the QR.p neuroblast (open oval) and its descendants. The QR.p neuroblast is generated in the posterior half of the animal and then migrates to about position 10. It then ceases to migrate and divides. One of the QR.p descendants undergoes programmed cell death (X) and the other migrates to about position 7. It then divides to generate the SDQR and AVM neurons (closed ovals). Figure 9A is based on Sulston and Horvitz [25]. B. AVM positions in EA485 and TU2562. The average position for 100 AVMs in both EA485 and TU2562 was 6.3. The AVM positions were measured as described in Figure 1.

ALM neurons so these neurons can be easily distinguished. In EA489, the BDUs were present even in animals with ALMs anterior to position 3 and they were located in their normal positions. The average position of BDUs in EA489 was 3.3 (n=50). The average position of BDUs in EA363 was 3.6 (n=50). Thus, the ALM/BDU cell divisions were taking place and the BDUs were migrating normally in these strains.

The migration defect was cold sensitive

To determine whether the ALM migration defect was sensitive to temperature, we grew EA471 and TU2562 at 15°C, 20°C and 25°C. We then measured the positions of the ALMs in each strain grown at each temperature. EA471 (a strain transformed with pJC3) was chosen because it showed an intermediate distribution of ALM positions at 20°C (see Figure 4), so either an anterior or a posterior shift would be apparent. TU2562 was chosen because its ALMs migrated close to their normal positions at 20°C.

Figure 9 shows the distribution of ALM positions for each strain at each temperature. The temperature at which the animals were grown affected ALM migrations in both EA471 and TU2562. ALMs were located more anteriorly in both EA471 and TU2562 grown at 15°C. TU2562 grown at 25°C had fewer ALMs anterior to position 9 than TU2562 grown at 20°C.

Discussion

We have identified a sequence in the *mec-3* upstream region that, when present in high copy extrachromosomal

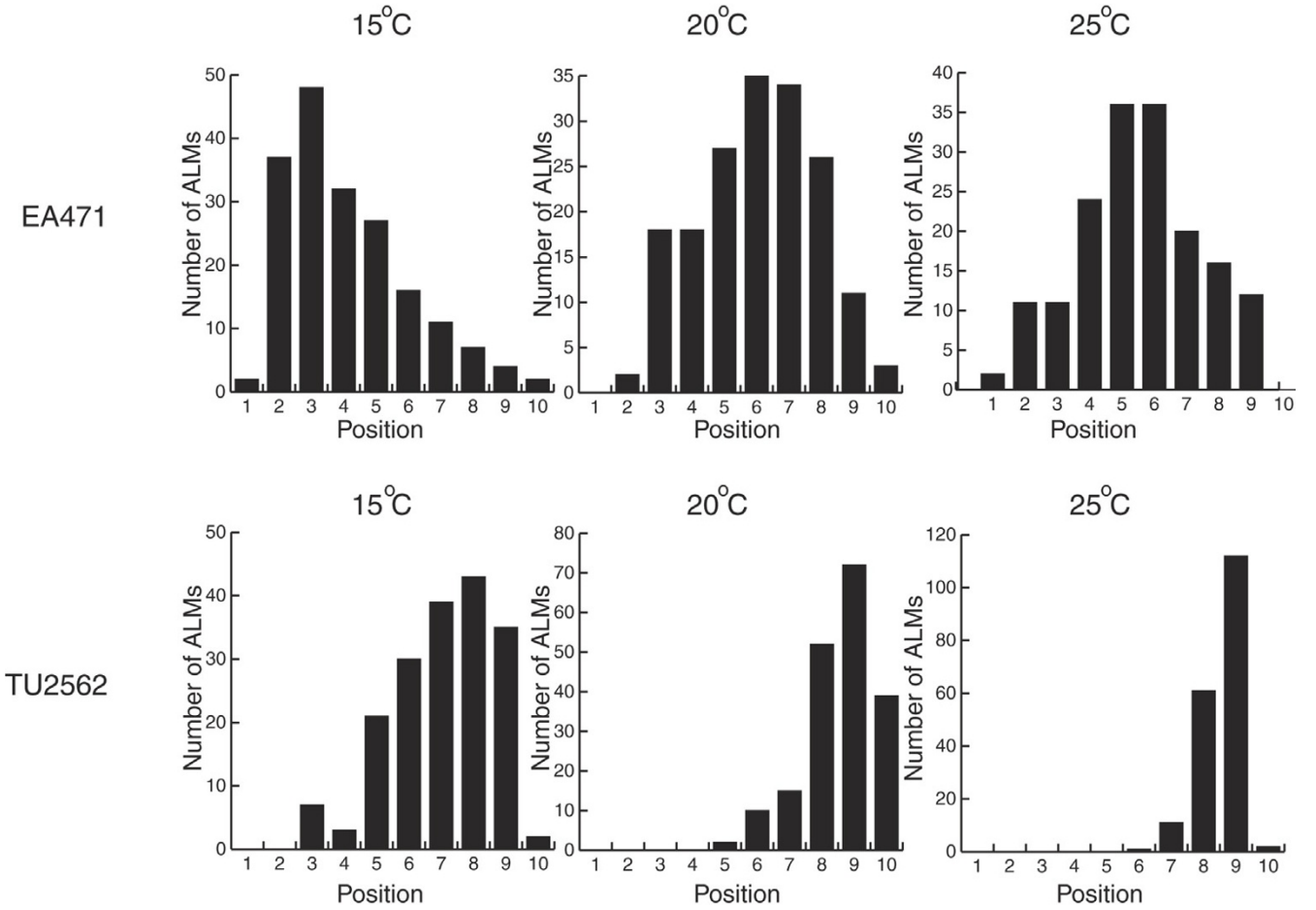

Figure 9
The effect of temperature on the ALM migration defect. Strains EA471 and TU2562 were grown at 15°C, 20°C and 25°C for more than a generation and the number of ALMs at each position was measured in 100 animals as described in Figure 1.

arrays, caused the ALM touch receptor neurons to migrate aberrantly and caused PLM touch receptor neuron axonal defects. These defects were not due to RNAi, non-specific effects of carrying a transgenic array, expression of GFP, or the marker gene used to make the transformants. Rather, these defects resulted from transgenic arrays containing many copies of a specific sequence from the *mec-3* upstream control region.

Figure 1A shows the direction and extent of the ALM and BDU cell migrations. ALMs that failed to migrate would remain around position 5 [12]. In strains transformed with the titrating sequence, the ALMs often migrated anteriorly rather than posteriorly and were located anterior to position 5. Thus, the arrays appeared to be sequestering a factor that controls both the direction and extent of ALM migrations. Presumably, the BDU neurons normally inherit a small amount of this factor and migrate anteriorly, while the ALMs inherit a larger amount of this factor and migrate posteriorly.

All ALMs that showed defects in axon morphology were anterior to position 6. Perhaps ALMs positioned anterior to position 6 sometimes fail to find their normal axon guidance cues. Interestingly, some of these anteriorly positioned ALMs had axon morphologies similar to BDU neurons. These cells, being deprived of their own axon guidance cues, may have followed the BDU axon guidance cues.

Figure 4 shows that the sequence upstream of the *Pst*I restriction site appeared to contribute strongly to the ALM migration defects. Plasmids containing this sequence (pJC8, pJC3 and pJC4) induced many ALM migration defects, whereas plasmids lacking this sequence (pPD118.17 and pJC1) induced few migration defects. Figure 6 shows that this upstream *mec-3* sequence alone (pJC10) was sufficient to induce migration defects. Smaller pieces of the sequence upstream of the *Pst*I site are also sufficient to induce ALM migration defects (Fig. 7). The smallest sequence tested that caused the migra-

tion defects (pJC16, Fig. 7) contained only 157 bp upstream of the *Eco*RI restriction site.

These conclusions assume that the arrays generated for each construct have roughly the same number of copies of the titrating sequence. We controlled for strain-to-strain variability in the array size by discarding strains with low transmission frequencies (see Materials and Methods) and by combining the data from at least three independently generated strains transformed with each construct. Because the strain-to-strain variability was small, this assumption is probably valid.

Other sequences around the titrating sequence appeared to facilitate the binding of the factor or factors involved in controlling ALM cell migrations. For instance, plasmid pJC10, which contained more surrounding sequence, was more effective than pJC15. These surrounding sequences may contain additional binding sites for this factor or the migration factor may interact with other proteins that bind the *mec-3* upstream sequences. Thus, the binding of one factor might cooperatively facilitate the binding of other factors. Li et al. [26] identified a sequence upstream of *her-1* that phenocopied an *sdc* mutation when transformed into *C. elegans* in high copy arrays. They too found that several regions of the *her-1* upstream sequence contributed to the effect.

The results shown in Figure 7 suggest that a 104 bp sequence, $^{5'}$AAATCTCAAT-10-CTAAAAACAT-20-TTTTAGAACT-30-TTTTCAAAGA-40-TATGTTGAAT-50-TCTGGCAACT-60-TTAGGTAGTT-70-TTAAATTTTC-80-CACGAAAT TT-90-CAAATC AAAT-1 00- GTTA$^{3'}$, contributed strongly to the ALM migration defects. The region from nucleotide 39-96 is a degenerate palindrome. Within this palindrome there are two more levels of nested palindromes. For instance, the 69-96 region is palindromic, and within the 69-96 region, the 84-96 region is palindromic.

Some of this interesting sequence structure may result from the juxtaposition of transcription factor binding sites. For instance, the sequence from 72-92 would be an excellent binding site in both its forward and reverse orientations for the *Drosophila* STAT transcription factor D-STAT [27]. There are two proteins with homology to the STAT family of transcription factors in *C. elegans*. This sequence is followed by the repeated sequence caaatcaaat, which would provide two good binding sites for the mammalian brain POU transcription factor Brn-2 [28]. Brn-2 is related to UNC-86, which is required to initiate and sustain *mec-3* expression.

The titrating sequence is located between two genes that are positioned head-to-head, *mec-3* and F01D4.1, which encodes a UDP-glucoronosyltransferase. The titrating element could be regulating either, neither, or both of these genes. Because this element appeared to sequester a factor involved in ALM migration and PLM axon outgrowth, it is probably a *mec-3* control element.

mec-3gfp fusion genes that lack this element appear to be correctly expressed. What aspect, then, of *mec-3* expression is affected by this control element? *mec-3* is activated by UNC-86 protein [13,14,15]. Once MEC-3 protein is made, UNC-86 and MEC-3 form a heterodimer that more effectively activates *mec-3*. Perhaps the titrating element is involved in the initial *mec-3* activation. This role would not be apparent in *mec-3gfp* fusion genes because they would be activated by the endogenous UNC-86/MEC-3 heterodimer. Alternatively, this element might help sustain *mec-3* expression. Finally, this element might modulate *mec-3* expression in a way that is not evident by looking at the MEC-3GFP fluorescence.

Figure 5 demonstrates that the ALM migration defect arises due to having many copies of the titrating sequence. Arrays made with few copies of pJC4 did not induce ALM migration defects, whereas arrays containing many copies of pJC4 did, thus suggesting that the arrays that altered ALM cell migrations acted by titrating a control factor.

It is somewhat surprising that high copy arrays could titrate this factor to low enough levels to induce phenotypes. Transgenic arrays in *C. elegans* contain about 50-100 copies of the plasmids used to make the array [29]. Assuming that each copy of the titrating sequence bound only one molecule, then shifting the concentration of this DNA binding factor by as few as 100 molecules caused the ALM migration defects. Because this factor is titratable, it may be present at low concentrations and bind with high affinity to the *mec-3* upstream sequence.

Perhaps this factor is present at low concentration because it is part of a mechanism for sensitive regulation of a cell state. The relative level of a factor present at low concentration should be easier to change than that of a factor present at high concentration. These results suggest that ALM migrations are carefully regulated by the concentration of a specific DNA binding protein that is present in the cell in only a few copies.

The need for an all-or-nothing response could also explain why there appear to be multiple sequences that contribute to the titration. One mechanism for steepening the response of an effector molecule is to require that more than one molecule bind to the target to induce a response. Perhaps the migration factor binds to several

sites in both *mec-3* and in the cell migration genes, and multiple sites must be bound to affect expression.

The factor sequestered by the titrating sequence does not affect all cell migrations. The AVM touch receptor neurons in EA485, a strain which showed a strong ALM migration defect, were located in the same position as the AVMs in TU2562, a strain which showed few ALM migration defects (Fig. 8). The AVM's lineal mother and grandmother both migrate anteriorly and if either of these migrations were defective, the AVMs would be mispositioned. We do not know whether other cell migrations were affected by the titrating sequence, but no other phenotypes were observed in animals with severe ALM migration defects.

The incidence of PLM axonal defects correlated well with the ALM migration defects. We believe, therefore, that the PLM defects were induced by titration of the same factor or factors that control ALM migrations. In both cases, the cells failed to correctly interpret anterior-posterior spatial information. However, the ALMs migrated to more anterior positions, whereas the PLMs axons often terminated at more posterior positions.

Temperature had a strong effect on the ALM migration defects (Fig. 9). In cells grown at lower temperatures, the titrated factor may be less active, it may be produced at low concentrations, it may bind to arrays more tightly, or it may interact with its ligand less effectively. The cold sensitivity of the ALM migration defect may be useful for identifying genetic suppressors of the migration defect.

The factor titrated by this sequence may also be involved in differentiating ALMs and BDUs. It may be present in AB.arpppapp and AB.arppaapp, the progenitors of ALMR/BDUR and ALML/BDUL, respectively. When these cells divide to generate ALMs and BDUs, the factor may differentially segregate into the ALMs. A high concentration of this factor may direct the ALMs to migrate posteriorly while a low level of this factor may direct the BDUs to migrate anteriorly. Furthermore, this factor may help activate *mec-3* expression and thereby cause the ALMs to differentiate into touch receptor neurons.

As was true in sea urchin embryos [30, 31], titration of transcription factors with high copy transgenes may be useful for characterizing control elements in *C. elegans*. The ALM migration defect should be useful for identifying optimal conditions for the titration of DNA binding protein with high copy arrays. We do not know, at this point, how often transcription factors will be present at low enough concentrations and bind DNA with enough affinity to apply this approach. Because others have also reported competitive titration by transgenic sequences in *C. elegans* [26, 32], we expect that it will not be uncommon. Certainly, some of the artifacts associated with transformation of *C. elegans* with high copy arrays may result from titration of DNA binding factors [23]. Transformation of *C. elegans* with low copy arrays made with complex carrier DNA prevented the titration effects, so the use of low copy arrays may be prudent where titration effects are not desired.

Kelly et al. [24] found that inclusion of complex carrier DNA in *C. elegans* transformation experiments improves the function of certain co-injected reporter constructs. These effects include both increased expression and improved uniformity of transgene expression. Figure 5 shows that including complex carrier DNA may also prevent transformation artifacts resulting from titration of transcription factors.

Conclusions

The experiments described here show that transformation of *C. elegans* with many copies of a specific sequence located upstream of *mec-3* induced cell migration and axonal guidance defects. This *mec-3* upstream sequence appeared to be sequestering a factor involved in controlling ALM migration and PLM axonal outgrowth. This factor may also regulate *mec-3* and thereby control touch receptor neuron fate. Titration of transcription factors with high copy arrays may become widely applicable in *C. elegans* once conditions that optimize this effect are found. The ALM defect described here may be useful for finding these conditions.

Materials and Methods

Worm culture and strain methods

C. elegans were maintained as described by Brenner [33]. Animals were grown at 20°C unless otherwise stated. The wild type strain was N2 var. Bristol. Strain TU2562, *mec-3gfp*(uIs22), was a gift from M. Chalfie.

Plasmid constructs

Standard molecular biology methods were used in making the following plasmids [34]. To make pJC1, we removed a *Pst*I-*Bbs*I fragment from pPD118.17, a gift from A. Fire. To make pJC3, we subcloned the *Nsi*I-*Pst*I fragment (1246 bp) of pTU23 [35] into the *Pst*I site of pPD118.17. We made pJC4 by deleting the *Pst*I-*Bbs*I fragment (1329 bp) from pJC3.

We made pJC8 from pBS1 and pJC3. To make pBS1, the oligonucleotides $^{5'}$ACCTCCCAAACTATAGATTGGGTG$^{3'}$ and $^{5'}$CGGCCAGAGTCGACTCACATATTG$^{3'}$ were used to amplify a 1370 bp fragment from pTU23. This introduced a *Sal*I site near the 3' end of the third exon of *mec-3*. We digested this fragment with *Hind*III and *Sal*I, and ligated it into the *Hind*III and *Sal*I sites of pPD95.67, a

gift from A. Fire. We removed the *Kpn*I-*Kpn*I fragment from pBS1 to make pBS1ΔK. We digested pBS1ΔK and pJC3 with both *Bbs*I and *Xho*I to remove a 1657 bp piece and a 908 bp piece, respectively. The remaining fragments were religated to make pJC8.

The only *mec-3* sequence in plasmid pJC10 was the 495 bp sequence 5' to the *Pst*I site. We constructed pJC10 by deleting the *Pst*I-*Nhe*I fragment (2861 bp) from pJC3. To make pJC11, we removed the *Not*I-*Nhe*I fragment (944 bp) from pJC4. Plasmid pJC12 was a *Hinc*II-*Hinc*II deletion (443 bp) of pJC10. To make pJC13, we removed the *Hinc*II-*Bgl*II fragment (602 bp) from pJC10. pJC14 was a *Hpa*I-*Bsp*EI deletion (309 bp) of pJC10, and pJC15 was a *Bgl*II-*Bsp*EI deletion (150 bp) of pJC10. To make pJC16, we digested pJC10 with *Bsp*EI and *Eco*RI to remove a 365 bp fragment. pJC17 was a *Bsp*EI-*Bsa*BI deletion (412 bp) of pJC10. pJC18 was a *Hinc*II-*Hinc*II deletion (443 bp) of pJC4, and pJC19 was a *Bsa*BI-*Bgl*II deletion (262 bp) of pJC4. All plasmids were prepared with the Wizard midiprep kit (Promega).

Transformation of C. elegans

Germ-line transformation was done as described by Mello et al. [29]. All constructs were co-injected with plasmid pRF4 containing the semidominant *rol-6(su1006)* allele, which causes a roller phenotype. Plasmids pJC1, pJC3, pJC4, and pJC8 were injected into N2 wild type animals at 100 μg/ml. Plasmids pJC10-pJC15 were injected into TU2562 at 100 μg/ml. Plasmid pRF4 was co-injected with all plasmids at 100 μg/ml.

To test whether the number of copies in the arrays had an effect on ALM migration, *Stu*I cut pJC4 was co-injected with *Sma*I cut pRF4 and *Pvu*II cut genomic DNA at the following concentrations (μg/ml): 2, 2, 100; 4, 4, 92; 8, 8, 84; 16, 16, 68; 32, 32, 36; 64, 32, 18; and 128, 32, 9, respectively. Larger arrays are transmitted to the next generation more effectively than smaller arrays [36]. All of the strains presented here had transmission frequencies greater than 16%.

Microscopy

Microscopy was done on an Olympus IMT-2 inverted microscope and on an Olympus AX70 microscope. A Power Mac G3 7100/80 with a frame grabber and IPlab software was used to collect and process images from the AX70. Both microscopes were equipped with fluorescence and Nomarski optics. Animals were immobilized with approximately 30 mM sodium azide and viewed at 100 X or 400 X.

RNAi

To make double stranded RNA for RNAi, we placed the *Pst*I-*Rsa*I fragment from pJC3 into pBluescript II KS+. RNA was made from the T3 and T7 promoters in pBluescript with a Maxiscript kit (Ambion). The dsRNA was injected at a concentration of 25 μg/ml.

Computer analysis

Sequence homologies were identified with the Blast algorithm [37, 38] at the National Center for Biotechnology Information (http://www.ncbi.nlm.nih.gov/). To identify long-range palindromic structures, an RNA secondary structure algorithm in the program DNASIS version 2.0 was used. Transcription factor binding sites were identified with MatInspector at http://genomatix.gsf.de/cgi-bin/matinspector/matinspector.pl [39].

Acknowledgements

This work was supported by grant RR10296 from the NIH. We thank Dr. M. Chalfie for strain TU2562 and Dr. A. Fire for plasmid pPD118.17. We thank Dr. Peter Good, Dr. Kelly Tatchell, Dr. Stephanie Aamodt and Dr. Joan McDermott for comments on an earlier draft of this manuscript. We are especially grateful to Dr. Kelly Tatchell for use of his Olympus AX70 microscope.

References

1. Cajal R: *Degeneration and Regeneration of the Nervous System. London: Oxford University Press;* 1928,
2. Montell DJ: **The genetics of cell migration in Drosophila melanogaster and Caenorhabditis elegans development.** *Development* 1999, **126**:3035-3046
3. Blelloch R, Newman C, Kimble J: **Control of cell migration during Caenorhabditis elegans development.** *Curr Opin Cell Biol* 1999, **11**:608-613
4. Hedgecock EM, Culotti JG, Hall DH: **The unc-5, unc-6 and unc-40 genes guide circumferential migrations of pioneer axons and mesodermal cells on the epidermis in C. elegans.** *Neuron* 1990, **2**:61-85
5. Hong K, Hinck L, Nishiyama M, Poo MM, Tessier-Lavigne M, Stein E: **A ligand-gated association between cytoplasmic domains of UNC5 and DCC family receptors converts netrin-induced growth cone attraction to repulsion.** *Cell* 1999, **97**:927-941
6. Bashaw GJ, Goodman CS: **Chimeric axon guidance receptors: the cytoplasmic domains of slit and netrin receptors specify attraction versus repulsion.** *Cell* 1999, **97**:917-926
7. Colavita A, Krishna S, Zheng H, Padgett RW, Culotti JG: **Pioneer axon guidance by UNC-129, a C. elegans TGF-beta.** *Science* 1998, **281**:706-709
8. Vincent S, Ruberte E, Grieder NC, Chen CK, Haerry T, Schuh R, Affolter M: **DPP controls tracheal cell migration along the dorsoventral body axis of the Drosophila embryo.** *Development* 1997, **124**:2741-2750
9. Wightman B, Clark SG, Taskar AM, Forrester WC, Maricq AV, Bargmann CI, Garriga G: **The C. elegans gene vab-8 guides posteriorly directed axon outgrowth and cell migration.** *Development* 1996, **122**:671-682
10. Wolf FW, Hung MS, Wightman B, Way J, Garriga G: **vab-8 is a key regulator of posteriorly directed migrations in C. elegans and encodes a novel protein with kinesin motor similarity.** *Neuron* 1998, **20**:655-666
11. Harris J, Honigberg L, Robinson N, Kenyon C: **Neuronal cell migration in C. elegans : regulation of Hox gene expression and cell position.** *Development* 1996, **122**:3117-3131
12. Sym M, Robinson N, Kenyon C: **MIG-13 positions migrating cells along the anteroposterior body axis of C. elegans.** *Cell* 1999, **98**:25-36
13. Lichtsteiner S, Tjian R: **Synergistic activation of transcription by UNC-86 and MEC-3 in Caenorhabditis elegans embryo extracts.** *EMBO J.* 1995, **14**:3937-3945
14. Xue D, Finney M, Ruvkun G, Chalfie M: **Regulation of the mec-3 gene by the C. elegans homeoproteins UNC-86 and MEC-3.** *EMBO J.* 1992, **11**:4969-4979

15. Xue D, Tu Y, Chalfie M: **Cooperative interactions between the Caenorhabditis elegans homeoproteins UNC-86 and MEC-3.** *Science* 1993, **261**:1324-1328
16. Chalfie M, Au M: **Genetic control of differentiation of the Caenorhabditis elegans touch receptor neurons.** *Science* 1989, **243**:1027-1033
17. Sulston JE, Schierenberg E, White JG, Thomson JN: **The embryonic cell lineage of the nematode Caenorhabditis elegans.** *Dev. Biol.* 1983, **100**:64-119
18. Jia Y, Xie G, Aamodt EJ: **pag-3, a C. elegans gene involved in touch neuron gene expression and coordinated movement.** *Genetics* 1996, **142**:141-147
19. Jia Y, Xie G, McDermott JB, Aamodt E: **The C. elegans gene pag-3 is homologous to the zinc finger proto-oncogene Gfi1.** *Development* 1997, **124**:2063-2073
20. Martinez-Serrano A, Villa A, Navarro B, Rubio FJ, Bueno C: **Human neural progenitor cells: better blue than green?** *Nat Med* 2000, **6**:483-484
21. Goldman S, Roy N: **Reply to "Human neural progenitor cells: better blue than green?".** *Nat Med* 2000, **6**:483-484
22. Fire A, Xu S, Montgomery MK, Kostas SA, Driver SE, Mello CC: **Potent and specific genetic interference by double-stranded RNA in Caenorhabditis elegans.** *Nature* 1998, **391**:806-811
23. McGhee JD, Krause MW: **Transcription factors and transcriptional regulation.** *In: C. ELEGANS II Edited by Riddle DL, Blumenthal T, Meyer BJ, Priess JR. pp. 147-184. Cold Spring Harbor: Cold Spring Harbor Laboratory Press;* 1997, 147-184
24. Kelly WG, Xu S, Montgomery MK, Fire A: **Distinct requirements for somatic and germline expression of a generally expressed Caenorhabditis elegans gene.** *Genetics* 1997, **146**:227-238
25. Sulston JE, Horvitz HR: **Post-embryonic cell lineages of the nematode Caenorhabditis elegans.** *Dev. Biol.* 1977, **56**:110-156
26. Li W, Streit A, Robertson B, Wood WB: **Evidence for multiple promoter elements orchestrating male-specific regulation of the her-1 gene in Caenorhabditis elegans.** *Genetics* 1999, **152**:237-248
27. Yan R, Small S, Desplan C, Dearolf CR, Darnell JE Jr: **Identification of a Stat gene that functions in Drosophila development.** *Cell* 1996, **84**:421-430
28. Li P, He X, Gerrero MR, Mok M, Aggarwal A, Rosenfeld MG: **Spacing and orientation of bipartite DNA-binding motifs as potential functional determinants for POU domain factors.** *Genes Dev* 1993, **7**:2483-2496
29. Mello CC, Kramer JM, Stinchcomb D, Ambros V: **Efficient gene transfer in C. elegans : extrachromosomal maintenance and integration of transforming sequences.** *EMBO J.* 1991, **10**:3959-3970
30. Livant DL, Hough-Evans BR, Moore JG, Britten RJ, Davidson EH: **Differential stability of expression of similarly specified endogenous and exogenous genes in the sea urchin embryo.** *Development* 1991, **113**:385-398
31. Franks RR, Anderson R, Moore JG, Hough-Evans BR, Britten RJ, Davidson EH: **Competitive titration in living sea urchin embryos of regulatory factors required for expression of the CyIIIa actin gene.** *Development* 1990, **110**:31-40
32. Carmi I, Kopczynski JB, Meyer BJ: **The nuclear hormone receptor SEX-1 is an X-chromosome signal that determines nematode sex.** *Nature* 1998, **396**:168-173
33. Brenner S: **The genetics of Caenorhabditis elegans.** *Genetics* 1974, **77**:71-94
34. Sambrook J, Fritsch EF, Maniatis T: *Molecular Cloning: A Laboratory Manual Second Edition. Cold Spring Harbor, New York: Cold Spring Harbor Laboratory Press;* 1989,
35. Way JC, Chalfie M: **mec-3, a homeobox-containing gene that specifies differentiation of the touch receptor neurons in C. elegans.** *Cell* 1988, **54**:5-16
36. Mello C, Fire A: **DNA transformation.** *Methods Cell Biol* 1995, **48**:451-482
37. Altschul SF, Gish W, Miller W, Myers EW, Lipman DJ: **Basic local alignment search tool.** *J. Mol. Biol.* 1990, **215**:403-410
38. Altschul SF, Madden TL, Schäffer AA, Zhang J, Zhang Z, Miller W, Lipman DJ: **Gapped BLAST and PSI-BLAST: a new generation of protein database search programs.** *Nucleic Acids Res.* 1997, **25**:3389-3402
39. Quandt K, Frech K, Karas H, Wingender E, Werner T: **MatInd and MatInspector - New fast and versatile tools for detection of consensus matches in nucleotide sequence data.** *Nucleic Acids Research* 1995, **23**:4878-4884